Compressive Tomographic Radar Imaging with Total Variation Regularization

Dehong Liu, Ulugbek S. Kamilov, and Petros T. Boufounos
Mitsubishi Electric Research Laboratories (MERL)
201 Broadway, Cambridge, MA 02139, USA
Email: {liudh, kamilov, petrosb}@merl.com

***Abstract*—We consider the problem of compressive imaging of a three-dimensional (3D) scene using multiple observations collected from parallel baselines, formed by monostatic sensors moving in space. In particular, we present a novel iterative imaging method based on the Omega-K algorithm with edge-preserving 3D total variation (TV) regularization. The method combines joint processing of multi-baseline data with TV minimization in a computationally efficient way, thus enabling high-resolution imaging of the reflectivity map of the scene. We demonstrate the potential of our method through numerical evaluations on simulated data with noise.**

***Keywords*—three-dimensional imaging, compressive sensing, high resolution imaging, total variation, omega-k imaging**

I. Introduction

It is well known that a linear array radar system is capable of imaging the two-dimensional (2D) range-azimuth reflectivity of an area by transmitting pulse signals and processing the corresponding echoes from the area. The resolution of the generated image in the range direction, which is perpendicular to the linear array, is determined by the bandwidth of the transmitted pulse, while the resolution in the azimuth or cross range direction, which is along the linear array, is inversely proportional to the aperture size. The linear array can be formed with a physical array composed of multiple physical elements with uniform spacing or a virtual array formed by a moving element. However, due to the lack of elevation aperture of a single baseline, such 2D imaging systems cannot capture elevation information of the scene.

In order to perform three-dimensional (3D) imaging of an area, observations from multiple baselines are necessary to form an elevation aperture. Similar to the azimuth direction, the elevation resolution is inversely proportional to the elevation aperture size. This fundamental limit in resolution leads to important considerations when designing state-of-the-art 3D imaging systems. For example, a practical realization of multiple baselines requires a large number of sensors in a physical array or several passes over the area for forming a virtual array. This makes the data collection an expensive and time consuming task. Additionally, physical considerations, such as, for example, the tight orbital tubes of the TerraSAR-X [1] and the COSMO-Skymed [2] systems, might further limit the realizable elevation aperture and the number of practically possible baselines. The small elevation aperture typically results in an elevation resolution that is much lower compared to that of range and azimuth. While recent sparsity-driven approaches [3] have significantly improved elevation resolution, the latter is still not comparable to the resolution achievable along range and azimuth directions.

In this paper, we re-examine the acquisition process and propose a novel computational imaging method that combines a novel multi-baseline measurement model with a sparsity-driven regularization based on 3D *total variation (TV)*. Our set-up considers monostatic radar platforms and assumes multi-baseline data from an area of interest collected by several radar platforms. Since platforms might be different, each baseline uses a fixed *pulse repetition frequency (PRF)* that could be different from the latter used in other baselines. Our formulation can handle arbitrarily baseline elevations within the available elevation space, which simplifies the data collection process. Thus, conventional tomographic radar imaging with multiple baselines reduces to a special case where only one platform is used in data collection. Our measurement model efficiently processes multi-baseline data in its entirety. Together with our fast iterative algorithm, it is possible to form high-resolution images in a computationally tractable fashion. The regularization with 3D TV further improves imaging process by effectively mitigating missing-data artifacts and suppressing noise while preserving edges in the image.

Our approach extends prior works [3]–[6] on 3D tomographic radar imaging by incorporating the following key contributions:

- Formulation of a model for joint processing of data from multiple radar platforms using different PRFs.
- Extension of previous work [6], which considered 3D imaging using planar baseline observations, to more general hyperplane observations.
- Development of a fast computational imaging method based on TV that substantially improves the final quality of reconstructed images.

Using the method described here, it is possible to form high-quality 3D reflectivity maps with a small number of baselines, directly reducing the time and cost necessary for data collection.

This paper is organized as follows. In Section II, we formulate our measurement model that is based on 3D Omega-K imaging. In Section III, we use the measurement model to develop the TV based reconstruction method. In Section IV, we validate our approach on simulated data.

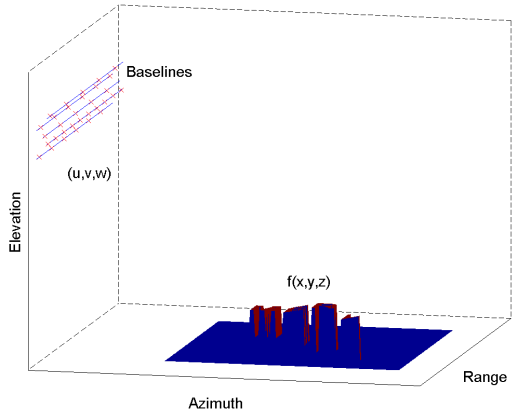

Fig. 1. Schematic representation of the scenario considered in this paper. A scene of reflectivity $f(\boldsymbol{r})$, $\boldsymbol{r} = (x, y, z) \in \mathbb{R}^3$, is illuminated from several monostatic radar platforms forming multiple parallel baselines. The echoes reflected from the scene are collected and jointly processed to computationally form an image of f.

II. Three-dimensional Omega-K Imaging

As summarized in Fig. 1, we consider a standard 3D radar imaging problem with a monstatic virtual array that is comprised of multiple platform trajectories, also referred to as baselines. We assume that all radar platforms operate in spotlight mode, which means that they illuminate the same area of interest. Each baseline forms a 2D image of the scene from a specific view angle. Conventional imaging systems, such as the ones used in TerraSAR-X or COSMO-Skymed, exploit stacks of complex-valued radar images from multiple passes—collected at different baselines and at different times—to form 3D images representing the reflectivity map of the scene [4]. Instead, in this paper, we treat the multi-baseline data jointly, to generate a high-resolution reflectivity map without the intermediate step of forming 2D image stacks. We assume for efficiency that all the baselines are parallel and aligned to each other. We also assume, without loss of generality, that all platforms use the same source pulse for illumination. We denote this pulse as $p(t)$ with the corresponding frequency spectrum

$$P(\omega) = \int_{\mathbb{R}} p(t) \mathrm{e}^{-\mathrm{j}\omega t} \, \mathrm{d}t, \tag{1}$$

where $\omega = 2\pi f$ represents the angular frequency.

In the monostatic scenario, the received echo that was reflected by the scene due to pulse p emitted at the location $\boldsymbol{r}' = (x', y', z')$ can be written as

$$s(\boldsymbol{r}', t) = \int_{\mathbb{R}^3} \frac{p\left(t - 2\frac{\|\boldsymbol{r} - \boldsymbol{r}'\|_{\ell_2}}{c}\right)}{4\pi \|\boldsymbol{r} - \boldsymbol{r}'\|_{\ell_2}} f(\boldsymbol{r}) \, \mathrm{d}\boldsymbol{r}, \tag{2}$$

where f is the ground reflectivity at location $\boldsymbol{r} = (x, y, z)$. The four-dimensional (4D), space-time, Fourier transform of the received echo can be expressed in the ω-$\boldsymbol{k}$ space as

$$S(\boldsymbol{k}', \omega) = \int_{\mathbb{R}^4} s(\boldsymbol{r}', t) \mathrm{e}^{-\mathrm{j}\langle \boldsymbol{k}', \boldsymbol{r}' \rangle - \mathrm{j}\omega t} \, \mathrm{d}\boldsymbol{r}' \, \mathrm{d}t, \tag{3}$$

where $\boldsymbol{k}' = (k'_x, k'_y, k'_z)$ is the wave vector, and $\langle \boldsymbol{k}', \boldsymbol{r} \rangle \triangleq k'_x x + k'_y y + k'_z z$. By using the method of *stationary phase* [7] and making the temporal origin correspond to the center $\boldsymbol{r}_0 = (x_0, y_0, z_0)$ of the 3D image, (3) can be expressed as

$$\begin{aligned} &S(\boldsymbol{k}', \omega) \\ &\quad = P(\omega) \frac{\mathrm{j}}{4k} \mathrm{e}^{-\mathrm{j}\langle \boldsymbol{k}, \boldsymbol{r}_0 \rangle + 2k\|\boldsymbol{r}_0\|_{\ell_2}} \int_{\mathbb{R}^3} f(\boldsymbol{r}) \mathrm{e}^{-\mathrm{j}\langle \boldsymbol{k}, \boldsymbol{r} \rangle} \, \mathrm{d}\boldsymbol{r} \\ &\quad = P(\omega) \frac{\mathrm{j}}{4k} \mathrm{e}^{-\mathrm{j}\langle \boldsymbol{k}, \boldsymbol{r}_0 \rangle + 2k\|\boldsymbol{r}_0\|_{\ell_2}} \mathcal{F}_{\text{3D}} \left\{ f(\boldsymbol{r}) \right\} (\boldsymbol{k}), \end{aligned} \tag{4}$$

where we set

$$k_y = k'_y, k_z = k'_z, k_x = \sqrt{4k^2 - (k'_y)^2 - (k'_z)^2} \tag{5}$$

with $k = \omega / c$. Here, the constant c denotes the speed of light and $\mathcal{F}_{\text{3D}}$ denotes the 3D Fourier transform.

The forward measurement process in (4), models the data acquisition as a function of the ground reflectivity in the ω-$\boldsymbol{k}$ space. Using (4) and the ground reflectivity, the radar echo can be efficiently computed with the fast Fourier transform (FFT). Additionally, we can express the reflectivity map f as the inverse Fourier transform of the collected raw data,

$$f(\boldsymbol{r}) = \mathcal{F}_{\text{3D}}^{-1} \left\{ \frac{-\mathrm{j}4kS(\boldsymbol{k}', \omega)}{P(\omega)} \mathrm{e}^{\mathrm{j}\langle \boldsymbol{k}, \boldsymbol{r}_0 \rangle - 2k\|\boldsymbol{r}_0\|_{\ell_2}} \right\}. \tag{6}$$

Thus, given sufficient amount of measurements, the 3D image of the ground reflectivity f can be efficiently formed by using the 3D inverse Fourier transform in the ω-$\boldsymbol{k}$ space. Note that, to use (6) for image formation, the data acquired over $(\boldsymbol{k}', \omega)$ first needs to be properly weighted and rearranged into a 3D data format over $\boldsymbol{k}$ according to the dispertion relation defined in (5) using a 3D Stolt mapping [8].

III. Imaging Method

A. Inverse Problem Formulation

Generally, high-resolution image formation with (6) requires a large elevation aperture and, correspondingly, large number of baselines with sufficiently high PRFs. Thus, high elevation resolution is often too expensive to achieve in practice due to constraints in elevation aperture size and the number of baselines.

We now describe a compressive imaging method, relying only on a small set of baselines, which enables reduction in the data acquisition burden. We start by discretizing (4) and representing it as a linear inverse problem

$$\mathbf{s} = \mathbf{H}\mathbf{f} + \mathbf{e}, \tag{7}$$

where the goal is to compute the unknown image $\mathbf{f} \in \mathbb{C}^N$ of ground reflectivities from the noisy, measured echoes $\mathbf{s} \in \mathbb{C}^M$. The measurement matrix $\mathbf{H} \in \mathbb{C}^{M \times N}$ models the linear operator (3) and can be efficiently computed with FFTs. The vector $\mathbf{e} \in \mathbb{C}^M$ represents the measurement noise. Due to compressive nature of the measurements, where $M < N$, the problem (7) is ill-posed. To circumvent this problem, we formulate image recovery as the regularized least-squares optimization

$$\widehat{\mathbf{f}} = \underset{\mathbf{f} \in \mathbb{C}^N}{\arg\min} \left\{ \frac{1}{2} \|\mathbf{s} - \mathbf{H}\mathbf{f}\|_{\ell_2}^2 + \lambda \mathcal{R}(\mathbf{f}) \right\}, \tag{8}$$

where $\lambda > 0$ is a parameter controlling the amount of regularization, and the functional $\mathcal{R}$ is the TV regularizer

$$\begin{aligned}\mathcal{R}(\mathbf{f}) &\triangleq \sum_{n=1}^{N} \|[\mathbf{D}\mathbf{f}]_n\|_{\ell_2} \\ &= \sum_{n=1}^{N} \sqrt{|[\mathbf{D}_x\mathbf{f}]_n|^2 + |[\mathbf{D}_y\mathbf{f}]_n|^2 + |[\mathbf{D}_z\mathbf{f}]_n|^2},\end{aligned} \tag{9}$$

where $\mathbf{D} : \mathbb{C}^N \to \mathbb{C}^{N\times 3}$ is the discrete gradient operator. The matrices $\mathbf{D}_x$, $\mathbf{D}_y$, and $\mathbf{D}_z$ denote the finite difference operators along the dimensions x, y, and z, respectively. The TV prior has been originally proposed by Rudin *et al.* [9] as a regularization approach capable of removing noise, while preserving image edges. It can be interpreted as a sparsity-promoting ℓ_1-penalty on the magnitudes of the image gradient and has proved to be successful in a wide range of applications in the context of sparse recovery of images from incomplete or corrupted measurements [10]–[14].

B. Iterative Optimization

The minimization (8) with TV is a non-trivial optimization task. The challenging aspects are the massive quantity of data that typically needs to be processed and the non-smooth nature of the regularization term (9).

We now design an efficient minimization scheme that can avoid both of these challenges. In particular, we consider an augmented-Lagrangian (AL) scheme [15], where we seek the critical points of the following cost

$$\begin{aligned}\mathcal{L}(\mathbf{f},\mathbf{d},\mathbf{z}) &\triangleq \frac{1}{2}\|\mathbf{s}-\mathbf{H}\mathbf{f}\|_{\ell_2}^2 + \lambda\sum_{n=1}^{N}\|[\mathbf{d}]_n\|_{\ell_2} \\ &\quad + \mathrm{Re}\{\mathbf{z}^{\mathrm{H}}(\mathbf{d}-\mathbf{D}\mathbf{f})\} + \frac{\rho}{2}\|\mathbf{d}-\mathbf{D}\mathbf{f}\|_{\ell_2}^2 \\ &= \frac{1}{2}\|\mathbf{s}-\mathbf{H}\mathbf{f}\|_{\ell_2}^2 + \lambda\sum_{n=1}^{N}\|[\mathbf{d}]_n\|_{\ell_2} \\ &\quad + \frac{\rho}{2}\|\mathbf{d}-\mathbf{D}\mathbf{f}+\frac{\mathbf{z}}{\rho}\|_{\ell_2}^2 - \frac{1}{2\rho}\|\mathbf{z}\|_{\ell_2}^2.\end{aligned}$$

Here,the superscript $^{\mathrm{H}}$ denotes the Hermitian transpose, $\mathbf{z} \in \mathbb{C}^{N\times 3}$ is the dual variable that imposes the constraint $\mathbf{d} = \mathbf{D}\mathbf{f}$, and $\rho > 0$ is the quadratic penalty parameter. The operator $\mathrm{Re}\{\mathbf{v}\}$ returns the real part of a complex vector $\mathbf{v}$. Traditional AL schemes solve (8) by alternating between a joint minimization step and an update step as

$$(\mathbf{f}^t,\mathbf{d}^t) \leftarrow \underset{\mathbf{f}\in\mathbb{C}^N,\mathbf{d}\in\mathbb{C}^{N\times 3}}{\arg\min} \left\{\mathcal{L}(\mathbf{f},\mathbf{d},\mathbf{z}^{t-1})\right\} \tag{10a}$$

$$\mathbf{z}^t \leftarrow \mathbf{z}^{t-1} + \rho(\mathbf{d}^t - \mathbf{D}\mathbf{f}^t). \tag{10b}$$

However, the joint minimization step (10a) can be computationally intensive. To get around this problem, we separate (10a) into a succession of simpler steps. This form of separation is commonly known as the alternating direction method of multipliers (ADMM) [16] and can be described as

$$\mathbf{f}^t \leftarrow \underset{\mathbf{f}\in\mathbb{C}^N}{\arg\min} \left\{\mathcal{L}(\mathbf{f},\mathbf{d}^{t-1},\mathbf{z}^{t-1})\right\} \tag{11a}$$

$$\mathbf{d}^t \leftarrow \underset{\mathbf{d}\in\mathbb{C}^{N\times 3}}{\arg\min} \left\{\mathcal{L}(\mathbf{f}^t,\mathbf{d},\mathbf{z}^{t-1})\right\} \tag{11b}$$

$$\mathbf{z}^t \leftarrow \mathbf{z}^{t-1} + \rho(\mathbf{d}^t - \mathbf{D}\mathbf{f}^t). \tag{11c}$$

By ignoring terms that do not depend on $\mathbf{f}$, the step (11a) can be expressed as linear filtering

$$\begin{aligned}\mathbf{f}^t &\leftarrow \underset{\mathbf{f}\in\mathbb{C}^N}{\arg\min}\left\{\frac{1}{2}\|\mathbf{s}-\mathbf{H}\mathbf{f}\|_{\ell_2}^2 + \frac{\rho}{2}\|\mathbf{D}\mathbf{f}-\mathbf{d}^{t-1}-\frac{\mathbf{z}^{t-1}}{\rho}\|_{\ell_2}^2\right\} \\ &\leftarrow \left(\mathbf{H}^{\mathrm{H}}\mathbf{H}+\rho\mathbf{D}^{\mathrm{H}}\mathbf{D}\right)^{-1}\left(\mathbf{H}^{\mathrm{H}}\mathbf{s}+\rho\mathbf{D}^{\mathrm{H}}(\mathbf{d}^{t-1}+\mathbf{z}^{t-1}/\rho)\right),\end{aligned}$$

which can be efficiently solved. Similarly, the step (11b) can be simplified as follows

$$\mathbf{d}^t \leftarrow \underset{\mathbf{d}\in\mathbb{C}^{N\times 3}}{\arg\min}\left\{\frac{1}{2}\|\mathbf{d}-\mathbf{q}^t\|_{\ell_2}^2 + \frac{\lambda}{\rho}\sum_{n=1}^{N}\|[\mathbf{d}]_n\|_{\ell_2}\right\},$$

with $\mathbf{q}^t \triangleq \mathbf{D}\mathbf{f}^t - \mathbf{z}^{t-1}/\rho$. This step is solved directly by component-wise application of the following shrinkage operator

$$\begin{aligned}\mathcal{T}(\mathbf{q};\tau) &\triangleq \underset{\mathbf{d}\in\mathbb{C}^3}{\arg\min}\left\{\frac{1}{2}\|\mathbf{d}-\mathbf{q}\|_{\ell_2}^2 + \tau\|\mathbf{d}\|_{\ell_2}\right\} \\ &= \max(\|\mathbf{q}\|_{\ell_2}-\tau,0)\frac{\mathbf{q}}{\|\mathbf{q}\|_{\ell_2}}.\end{aligned}$$

Thus, we can express (11b) as

$$[\mathbf{d}^t]_n \leftarrow \mathcal{T}([\mathbf{D}\mathbf{f}^t - \mathbf{z}^{t-1}/\rho]_n; \lambda/\rho),$$

for every $n = 1, 2, \ldots, N$.

To concluder, we described a method based on ADMM for iteratively minimizing the proposed objective functional. The algorithm allows us to reduce the optimization to a succession of straightforward operations.

IV. Experiments

In order to validate our approach, we simulated the data acquired via (4), and performed reconstruction using both conventional methods and the proposed one. In particular, as shown in Fig. 2(a) the scene corresponds to letters *MERL* comprised of point scatterers placed in a 3D space with different elevations. As shown in Fig. 1, we collect a total of 10 baselines, randomly selected from a total number of 1010 possible baselines, along 10×101 range-elevation grids. Raw radar data are collected from each baseline with a fixed PRF; however, for each baseline, the corresponding PRF is randomly selected. Specifically, starting from a reference PRF, all baselines have PRFs sub-sampled by a random integer amount. In other words, each PRF is a fraction of the reference PRF, with the downsampling rate randomly selected from the set $\{2, 3, 4, 5\}$. Considering the practical noise problem, we add white Gaussian noise to the simulated data with a peak-signal-to-noise (PSNR) ratio equal to 15 dB.

We compare three different methods: conventional reconstruction, image-domain sparsity-based reconstruction, and the proposed TV-based method. For conventional 3D imaging with reduced data collection, we use the ω-$\boldsymbol{k}$ imaging relationship (6) by upsampling the data and filling in missing data with zeros. This approach produces a fast delay-and-sum-type reconstruction from the acquired data implementing the adjoint (backprojection) of the acquisition operator. For image-domain sparsity-based method, we use iterative algorithm that was described in [6].

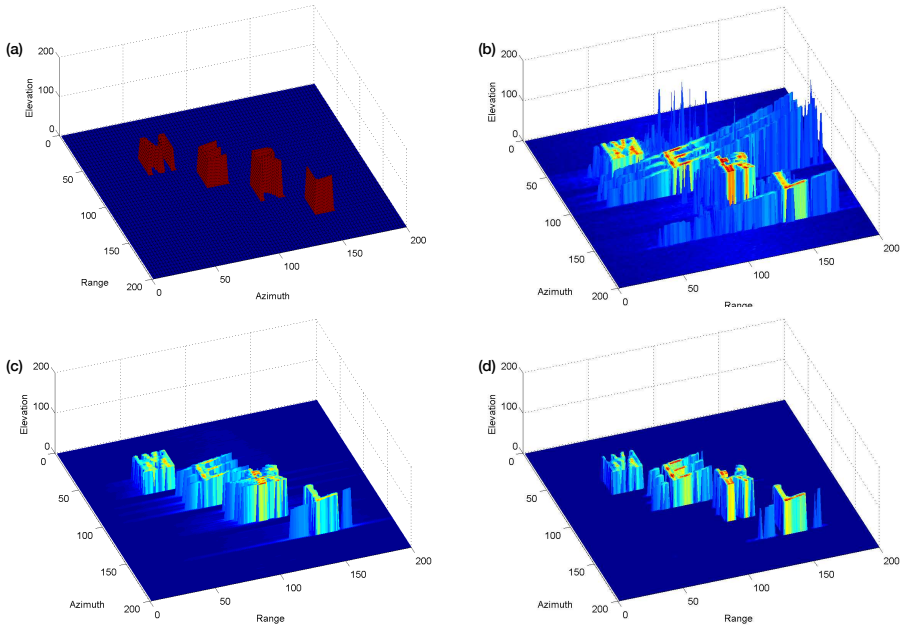

Fig. 2. Comparison of three image formation methods on a region of size $200 \times 200 \times 200$ voxels containing letters *MERL*. (a) True image. (b) Conventional image formation via (6). (c) Method based on image domain sparsity [6]. (d) Proposed method.

The imaging results are shown in Fig. 2(b)–(d), where from top to bottom, we plot the reflectivity of (b) conventional approach, (c) approach from [6], and (d) our proposed approach. The color intensity in the image represents the intensity of the recovered reflectivity. The results illustrate that in the compressive regime with limited data-collection, conventional linear methods produce degraded images that exhibit low resolution in both azimuth and elevation. Both sparsity-driven approaches significantly improve the reconstruction performance by removing missing-data artifacts. However, the proposed TV-based approach yields substantially better images compared to the one based on image-domain sparsity. In particular, one can observe that the the buildings recovered under TV have a desirable piecewise-smooth nature with sharp edges.

From computational perspective, the proposed reconstruction takes about 4 minutes per iteration for a $200 \times 200 \times 200$ 3D map using MATLAB on a 3.6 GHz Intel Xeon CPU, and requires less than 50 iterations for convergence.

To conclude, we presented a 3D TV-based compressive imaging method that fuses multi-baseline multi-PRF data from radar platforms. Imaging results on simulated data showed the potential of the method to recover 3D reflectivity maps of an area of interest when number of baselines is small.

REFERENCES

[1] German Aerospace Center (DLR), "TerraSAR-X," http://terrasar-x.dlr.de.

[2] Italian Aerospace Center (ASI), "COSMO-SkyMed," http://www.asi.it/en/activity/earth_observation/cosmoskymed.

[3] X. X. Zhu and R. Bamler, "Tomographic SAR inversion by L_1-norm regularization—the compressive sensing approach," *IEEE Trans. Geosci. Remote Sens.*, vol. 48, no. 10, pp. 3839–3846, October 2010.

[4] G. Fornaro, F. Serafino, and F. Soldovieri, "Three-dimensional focusing with multipass SAR data," *IEEE Trans. Antennas Propag.*, vol. 41, no. 3, pp. 507–517, March 2003.

[5] J. M. Lopez-Sanchez and J. Fortuny-Guasch, "3-D imaging using range migration techniques," *IEEE Trans. Antennas Propag.*, vol. 48(5), pp. 728–737, May 2000.

[6] D. Liu and P. T. Boufounos, "Compressive sensing based 3D SAR imaging with multi-PRF baselines," in *IEEE International Geoscience and Remote Sensing Symposium (IGARSS)*, 2014.

[7] M. Born and E. Wolf, *Principles of optics*. Cambridge University press, 1999.

[8] X. Zhuge and A. G. Yarovoy, "Three-dimensional near-field MIMO array imaging using range migration techniques," *IEEE Trans. Image Processing*, vol. 21(6), pp. 3026–3033, June 2012.

[9] L. I. Rudin, S. Osher, and E. Fatemi, "Nonlinear total variation based noise removal algorithms," *Physica D*, vol. 60, no. 1–4, pp. 259–268, November 1992.

[10] M. M. Bronstein, A. M. Bronstein, M. Zibulevsky, and H. Azhari, "Reconstruction in diffraction ultrasound tomography using nonuniform FFT," *IEEE Trans. Med. Imag.*, vol. 21, no. 11, pp. 1395–1401, November 2002.

[11] M. V. Afonso, J. M.Bioucas-Dias, and M. A. T. Figueiredo, "Fast image recovery using variable splitting and constrained optimization," *IEEE Trans. Image Process.*, vol. 19, no. 9, pp. 2345–2356, September 2010.

[12] E. J. Candès, J. Romberg, and T. Tao, "Robust uncertainty principles: Exact signal reconstruction from highly incomplete frequency information," *IEEE Trans. Inf. Theory*, vol. 52, no. 2, pp. 489–509, February 2006.

[13] M. Lustig, D. L. Donoho, and J. M. Pauly, "Sparse MRI: The application of compressed sensing for rapid MR imaging," *Magn. Reson. Med.*, vol. 58, no. 6, pp. 1182–1195, December 2007.

[14] U. S. Kamilov, I. N. Papadopoulos, M. H. Shoreh, A. Goy, C. Vonesch, M. Unser, and D. Psaltis, "Optical tomographic image reconstruction based on beam propagation and sparse regularization," *IEEE Trans. Comp. Imag.*, vol. 2, no. 1, pp. 59–70,, March 2016.

[15] J. Nocedal and S. J. Wright, *Numerical Optimization*, 2nd ed. Springer, 2006.

[16] S. Boyd, N. Parikh, E. Chu, B. Peleato, and J. Eckstein, "Distributed optimization and statistical learning via the alternating direction method of multipliers," *Foundations and Trends in Machine Learning*, vol. 3, no. 1, pp. 1–122, 2011.